By substitution into Eq. (8), the unknown displacements are

$$p_1 = D_{00}P_0 + D_{01}D_{11}^{-1}(p_0 - D_{10}P_0) \quad (11)$$

Noting that

$$b = \{b_1b_2 \ldots b_g \ldots\}$$
$$S = \{S_1S_2 \ldots S_g \ldots\}$$
$$w = \{w_1w_2 \ldots w_g \ldots\}$$
$$f = \lceil f_1f_2 \ldots f_g \ldots \rfloor$$

then, from Eq. (1), considering all of the elements,

$$S = bP = b_0P_0 + b_1D_{11}^{-1}(p_0 - D_{10}P_0) \quad (12)$$

and, similarly,

$$w = fS = fb_0P_0 + fb_1D_{11}^{-1}(p_0 - D_{10}P_0) \quad (13)$$

As D equals $b'fb$, then

$$D_{00} = b_0'fb_0 = \Sigma b_{0g}'f_g b_{0g}$$
$$D_{01} = b_0'fb_1 = \Sigma b_{0g}'f_g b_{1g}$$
$$D_{10} = b_1'fb_0 = \Sigma b_{1g}'f_g b_{0g}$$
$$D_{11} = b_1'fb_1 = \Sigma b_{1g}'f_g b_{1g}$$

By substitution into Eq. (8), the unknown forces are

$$R_1 = C_{00}r_0 + C_{01}C_{11}^{-1}(R_0 - C_{10}r_0) \quad (11)$$

Noting that

$$a = \{a_1a_2 \ldots a_g \ldots\}$$
$$v = \{v_1v_2 \ldots v_g \ldots\}$$
$$T = \{T_1T_2 \ldots T_g \ldots\}$$
$$k = \lceil k_1k_2 \ldots k_g \ldots \rfloor$$

then, from Eq. (1), considering all of the elements,

$$v = ar = a_0r_0 + a_1C_{11}^{-1}(R_0 - C_{10}r_0) \quad (12)$$

and, similarly,

$$T = kv = ka_0r_0 + ka_1C_{11}^{-1}(R_0 - C_{10}r_0) \quad (13)$$

As C equals $a'ka$, then

$$C_{00} = a_0'ka_0 = \Sigma a_{0g}'k_g a_{0g}$$
$$C_{01} = a_0'ka_1 = \Sigma a_{0g}'k_g a_{1g}$$
$$C_{10} = a_1'ka_0 = \Sigma a_{1g}'k_g a_{0g}$$
$$C_{11} = a_1'ka_1 = \Sigma a_{1g}'k_g a_{1g}$$

It may be noticed that, for a structure under either applied forces or imposed displacements, Eqs. (10–13) will reduce to those that Argyris derived by a different approach.

References

[1] Ostenfeld, A., *Die Deformationsmethode* (Springer-Verlag, Berlin, Germany, 1926).

[2] Argyris, J. H., "Energy theorems and structural analysis," Aircraft Eng. 26, 347 (1954).

Hypersonic Sharp-Leading-Edge Problem for Axially Symmetric Bodies

Jay M. Solomon*
U. S. Naval Ordnance Laboratory, White Oak, Silver Spring, Md.

During the past several years, the so-called hypersonic sharp-leading-edge problem has been the subject of several investigations. All of these have been concerned with the particular case of a flat plate at zero incidence. The present note applies some of the methods developed for the flat plate to other bodies, in particular to pointed bodies of revolution at zero incidence. The present analysis is based on the viscous-layer model used by Oguchi[1] in his first analysis of the sharp-leading-edge problem. Essentially, Oguchi[1] assumes that 1) all rarefaction effects very near the tip are negligible; 2) the undisturbed flow is separated from the disturbed flow by a thin, nearly straight shock wave, which is attached at the leading edge and which satisfies the oblique shock relations; and 3) the flow behind the leading-edge shock wave forms a continuum viscous layer, which is sufficiently thin so that the Navier-Stokes equations can be truncated to their boundary-layer form.

Because of these simplifications, Oguchi's results show some inconsistencies[3, 4] (as do the results of Jain and Li[2] and Bendor[3] which also employ Oguchi's model). However, these analyses yield surface pressures very near the leading edge which are considerably more realistic than those predicted using strong interaction theory. Herein lies the justification for applying Oguchi's ideas to pointed-nose bodies of revolution.

Analysis

Longitudinal curvature effects throughout the layer are assumed negligible. Furthermore, the gas is assumed to be perfect and to have constant c_p and Pr.† By the forementioned assumption 3, the applicable equations are the boundary-layer equations that include transverse curvature terms [e.g., Eqs. (1.2–1.5, 1.8, and 1.9) of Ref. 5]. These equations are obtained from the full Navier-Stokes and energy equations by neglecting terms of the order of Δ/L, where Δ is of the order of the viscous-layer thickness, and L is of the order of the viscous-layer length. By assumption 2, the dependent variables u, v, p, ρ, and H must attain the values u_s, v_s, p_s, ρ_s, and H_s,‡ respectively, at some unknown but finite shock-wave distance $y_s(x)$. Furthermore, the values u_s, v_s, etc. are given by the oblique shock relations and hence depend on M_∞ and the local shock-wave angle ψ. Note that, neglecting longitudinal curvature, ψ is related to y_s by

$$dy_s/dx = \tan(\psi - \alpha) \quad (1)$$

For hypersonic conditions (i.e., $M_\infty \gg 1$), the oblique shock relations indicate that

$$v_s = u_\infty[(1 - \gamma)\sin\alpha + 2\sin(\psi - \alpha)\cos\psi]/(\gamma + 1) \quad (2)$$

† The coordinate system and notation used herein will agree with that of Yasuhara[5] except where otherwise defined.

‡ The subscript s will herein denote quantities evaluated directly behind the shock wave.

Received January 4, 1965.

* Research Aerospace Engineer.

whereas the thin-layer analysis indicates that $v_s/u_\infty \sim 0(\Delta/L)$. Since longitudinal curvature is neglected, $(\psi - \alpha) \sim 0(\Delta/L)$; thus, in order to make Eq. (2) consistent with the thin-layer assumption, it must be assumed that $(\gamma - 1)\sin\alpha/(\gamma + 1) \sim 0(\Delta/L)$, which is to be verified a posteriori. In the present analysis, it will be convenient to replace Eq. (2) by the "over-all" mass conservation equation, viz.,

$$\rho_\infty u_\infty r_s^2 = 2\int_0^{y_s} r\rho u\, dy \tag{3}$$

Thus, the system of equations to be solved consists of Eqs. (1.2–1.4 and 1.8) of Ref. 5 along with Eq. (3), subject to the surface conditions $u(x, 0) = 0$, $v(x, 0) = 0$, $H(x, 0) = H_w(x)$, and the shock conditions (for $M_\infty \gg 1$)

$$\left.\begin{aligned} u(x, y_s) &= u_\infty \cos\alpha \\ p(x, y_s) &= 2\gamma p_\infty M_\infty^2 \sin^2\psi/(\gamma + 1) \\ T(x, y_s) &= 2\gamma(\gamma - 1)T_\infty M_\infty^2 \sin^2\psi/(\gamma + 1)^2 \\ H(x, y_s) &= H_\infty \end{aligned}\right\} \tag{4}$$

In the first expression of Eq. (4), terms of order $u_\infty(\psi - \alpha)\sin\alpha$ have been neglected. It can be shown[4] that the resulting value for v_s obtained from this system agrees up to the order $(\psi - \alpha)^2$ with that given by Eq. (2).

The analysis will be sketched now under the additional assumptions $\mu \propto T^\omega(\frac{1}{2} \leq \omega \leq 1)$, H_w = const, and $Pr = 1$. (For a more detailed description, see Ref. 4.) Following Oguchi's analysis, a boundary-layer local similarity-type transformation is performed; i.e., the new independent variables are defined by

$$\begin{aligned} \xi &= u_\infty \int_0^x \rho_w\mu_w r_w^2 \cos\alpha dx \\ \eta &= \frac{(u_\infty \cos\alpha)}{(2\xi)^{1/2}} \int_0^y \rho r \quad dy \end{aligned} \tag{5}$$

and the new dependent variables are defined by§

$$f_\eta = u/(u_\infty \cos\alpha) \qquad \Theta = (H - H_w)/(H_\infty - H_w) \tag{6}$$

A final transformation given by

$$X = \xi^{1/3} \qquad Y = \eta/\eta_s \qquad F = f/\eta_s \tag{7}$$

reduces the differential equations to the following form:

$$\left.\begin{aligned} \mathfrak{D}[F_Y] &= \eta_s^2 \left\{\frac{(\gamma - 1)\lambda\mathfrak{B}[\sin^2\psi]}{2\gamma \cos^2\alpha} + (F_Y)^2\mathfrak{B}[\cos\alpha]\right\} \\ \mathfrak{D}[\Theta] &= 0 \end{aligned}\right\} \tag{8}$$

In the preceding, $\lambda \equiv c_pT/H_\infty = \lambda_w + (1 - \lambda_w)\Theta - (F_Y)^2 \cos^2\alpha$, and the operators $\mathfrak{D}$ and $\mathfrak{B}$ are defined by

$$\mathfrak{D}[h] \equiv [(1 + \zeta P)Nh_Y]_Y - \eta_s^2\{\tfrac{2}{3}X(F_Yh_X - F_Xh_Y) + (\mathfrak{B}[\eta_s] - 1)Fh_Y\}$$

$$\mathfrak{B}[h] \equiv (2X/3h)(dh/dX)$$

where

$$N \equiv \frac{\rho\mu}{\rho_w\mu_w} = \left(\frac{\lambda}{\lambda_w}\right)^{\omega - 1} \qquad P \equiv \int_0^Y \lambda\, dY$$

$$\zeta \equiv \frac{(\gamma^2 - 1)(2\xi)^{1/2}\eta_s}{2\gamma\rho_\infty u_\infty r_w^2 \sin^2\psi}$$

Equation (3) is transformed into

$$\frac{1 + \zeta P(X, 1)}{F(X, 1)} = \frac{2(2\xi)^{1/2}\eta_s}{\rho_\infty u_\infty r_w^2} = \frac{4\gamma\zeta \sin^2\psi}{\gamma^2 - 1} \tag{9}$$

§ An independent variable used as a subscript will denote partial differentiation with respect to that variable.

The boundary conditions become $F(X, 0) = F_Y(X, 0) = 0$, $F_Y(X, 1) = 1$, $\Theta(X, 0) = 0$, $\Theta(X, 1) = 1$. The parameter ζ is the transverse curvature parameter for the viscous layer.[4]

Consider now the asymptotic solution of the original system near $x = 0$ (as suggested by Jain and Li[2] and Bendor[3] for the flat-plate problem). The bodies being considered are assumed given in the form $r_w = r_1x + 0(x^2)$ or $\alpha = \alpha_0 + 0(x)$ with $0 < \alpha_0 < 90°$; also, since the shock wave is assumed attached at the tip, it has the form $\psi = \psi_0 + 0(x)$ with $\alpha_0 \leq \psi_0 \leq 90°$. Therefore, by Eqs. (5) and (7), $X = cx + 0(x^2)$, where c is a positive constant. The transformed system is thus to be considered near $X = 0$. Equations (8) and (9) and the boundary conditions suggest the following expansions about $X = 0$:

$$\left.\begin{aligned} &F(X, Y) = F_0(Y) + F_1(Y)X + \ldots \\ &\Theta(X, Y) = \Theta_0(Y) + \Theta_1(Y)X + \ldots \\ &\zeta(X) = \zeta_0 + \zeta_1X + \ldots \qquad \eta_s^2(X) = \eta_1X + \ldots \\ &\psi(X) = \psi_0 + \psi_1X + \ldots \end{aligned}\right\} \tag{10}$$

Only the leading terms will be considered herein.

Substitution of Eq. (10) into Eqs. (8) and (9) yields the following system for the leading terms:¶

$$\left.\begin{aligned} &[(1 + \zeta_0P_0)N_0F_0'']' = 0 \\ &[(1+ \zeta_0P_0)N_0\Theta_0']' = 0 \\ &F_0(0) = F_0'(0) = \Theta_0(0) = 0 \\ &F_0'(1) = \Theta_0(1) = 1 \end{aligned}\right\} \tag{11}$$

$$[1 + \zeta_0P_0(1)]/F_0(1) = 4\gamma\zeta_0 \sin^2\psi_0/(\gamma^2 - 1) \tag{12}$$

In the preceding, the quantities N_0 and P_0 are N and P, respectively, evaluated with F, Θ, and α replaced by their zero-order terms. In order to use Eq. (12), a relation between ψ_0 and the other transformed variables must be obtained. To do this, note that $[r_w + y_s \cos\alpha]^2 = r_w^2[1 + \zeta P(X, 1)]$. Differentiation of this and use of Eqs. (1) and (10) yield, for the leading terms, $\tan(\psi_0 - \alpha_0) = (\varphi - 1)\tan\alpha_0$ where $\varphi^2 \equiv 1 + \zeta_0P_0(1)$. This expression may be used to eliminate ψ_0 in Eq. (12) to obtain

$$\zeta_0 = \frac{(\gamma^2 - 1)\varphi^2 \cot^2\alpha_0}{4\gamma[\varphi^2 \cos(2\alpha_0) + 2\varphi \sin^2\alpha_0 - \sin^2\alpha_0]F_0(1)} \tag{13}$$

In order to obtain the preceding, the approximations $\tan(\psi_0 - \alpha_0) \approx \sin(\psi_0 - \alpha_0)$ and $\sin^2\psi_0 \approx \sin^2(\psi_0 - \alpha_0)\cos(2\alpha_0) + \sin(\psi_0 - \alpha_0)\sin(2\alpha_0) + \sin^2\alpha_0$, which are within the thin-layer approximation, were used.

Equation (11) indicates that $F_0' = \Theta_0$; hence, Θ_0 can be eliminated from Eq. (11). For fixed ζ_0, the integrodifferential equation for F_0 in Eq. (11) can be solved in the form

$$\beta Y(F_0') = \int_0^{F_0'} A^{\omega-1}(t) \exp\{\zeta_0C(t)/\beta\}dt \equiv I(F_0';\ \zeta_0, \beta) \tag{14}$$

where

$$C(t) = \int_0^t A^\omega(\tau)d\tau \qquad A(t) = \lambda_w + (1 - \lambda_w)t - t^2 \cos^2\alpha_0$$

and β is a constant of integration equal to $\lambda_w^{\omega-1}F_0''(0)$. The constant β is given implicitly by $\beta = I(1;\ \xi_0, \beta)$, which follows from Eq. (14), and the condition $Y(1) = 1$ [i.e., $F_0'(1) = 1$]. The quantities $F_0(1)$ and φ, which appear in Eq. (13), may be expressed as

$$F_0(1) = 1 - \int_0^1 Y(t)dt \qquad \varphi^2 = \exp\{\zeta_0C(1)/\beta\}$$

The latter is obtained by using $F_0''(0) = F_0''(1)N_0(1)$

¶ A prime indicates differentiation with respect to Y.

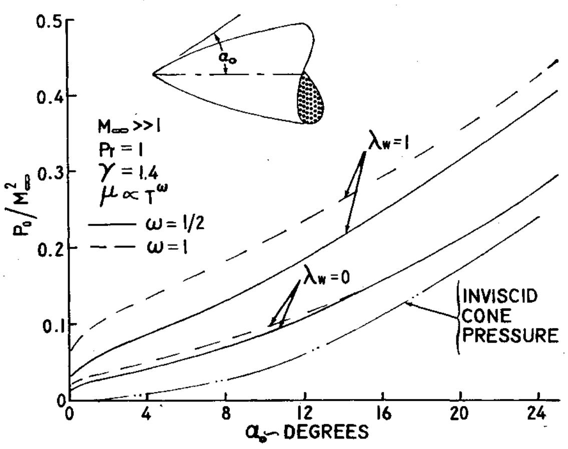

Fig. 1 Tip pressure ratio.

$\exp\{\zeta_0 C(1)/\beta\}$, which is Eq. (14) differentiated and evaluated at $F_0' = 1$, and $[1 + \zeta_0 P_0(1)]N_0(1)F_0''(1) = F_0''(0)$, which is the first expression in Eq. (11) integrated and evaluated at $Y = 1$. Equation (13) thus yields ζ_0 implicitly.

The principal result is the surface pressure. It is obtained from Eqs. (4) and (10) in the form $p_w/p_\infty = p_0 + 0(x)$ where, from Eqs. (4) and (12), $p_0 = (\gamma - 1)M_\infty^2\varphi^2/[2\zeta_0 F_0(1)]$. Some results for p_0 are shown in Fig. 1. A more complete presentation of results can be found in Ref. 4, which also includes some results for two-dimensional pointed-nosed bodies.

References

[1] Oguchi, H., "The sharp leading edge problem in hypersonic flow," *Rarefied Gas Dynamics* (Academic Press Inc., New York, 1961), Sec. 5, pp. 501–524.

[2] Jain, A. C. and Li, T. Y., "The problem of sharp leading edge in hypersonic flow," Aerospace Research Labs. Rept. ARL 63-161 (1963).

[3] Bendor, E., "Rarefied viscous flow near a sharp leading edge," AIAA J. 1, 956–958 (1963).

[4] Solomon, J. M., "On the hypersonic sharp leading edge problem for bodies other than flat plates," U. S. Naval Ordnance Lab. Rept. NOLTR 65-8 (to be published).

[5] Yasuhara, M., "Axisymmetric viscous flow past very slender bodies of revolution," J. Aerospace Sci. **29**, 667–679 (1962).

Switch-Triggered Pulsed Plasma Accelerator Thrust Measurements

William J. Guman*
Republic Aviation Corporation, Farmingdale, N. Y.

The electrical discharge in many pulsed plasma accelerators intended for space propulsion is initiated by injecting gaseous propellant into the interelectrode spacing of electrically charged electrode nozzles. Initiating an electrical discharge in this manner is frequently called "propellant-triggering." The advantage of this triggering technique is absence of a repetitive, fast-acting, high-current switch in the electrical network of the accelerator. However, propellant-triggered accelerators generally electromagnetically accelerate only a portion of the injected propellant. By introducing a switch into the electrical network it becomes possible to delay application of voltage relative to propellant injection and therefore to vary propellant utilization. This note presents experimental data showing that, with a switch-triggered pulsed plasma accelerator, it is possible to vary specific thrust even after the initial drop in thrust.[1]

During the propellant injection phase of a propellant-triggered accelerator, gaseous propellant expands across a valve seat and through injection ports into the evacuated interelectrode spacing of the electrode nozzle. The interelectrode gas pressure rises in the neighborhood of the injection ports, and an electrical discharge occurs during this pressure rise. Since the time-varying interelectrode pressure rises from a value below the pressure level corresponding to the low-pressure branch of a Paschen curve, the electrical discharge takes place with the breakdown voltage-pressure relationship represented by the equivalent of the low-pressure branch of a Paschen curve. Once the discharge is initiated, the mass distributed in the interelectrode spacing is swept out of the nozzle within a few microseconds. Because it is not possible to terminate propellant flow instantly, gaseous propellant usually continues to enter the interelectrode spacing after termination of the electrical discharge. It is neither possible to energize this "afterflow" of propellant, nor to inject, prior to the electrical discharge, an arbitrary quantity of mass having peak pressures near the high-pressure branch of the Paschen curve. An accelerator that uses a switch to delay application of voltage relative to propellant injection usually energizes some propellant "afterflow," besides making it possible for an arbitrary quantity of propellant, having an arbitrary peak interelectrode pressure, to be injected prior to the acceleration process. It must be noted, however, that switch-triggering offers no advantage over propellant-triggering if the maximum value of the injected time-varying interelectrode pressure is just equal to the minimum pressure required to initiate the electrical discharge by propellant-triggering (i.e., by shorting the switch). To utilize the advantages of switch-triggering, it is necessary to inject either more gaseous propellant, or gaseous propellant at a higher pressure, into a switch-triggered accelerator rather than into the same accelerator operated by propellant-triggering.

In the present study, a low-pressure, linear pinch-type switch was devised and inserted in series into the electrical circuit of a pinch-type pulsed plasma accelerator. The interelectrode spacing of the switch was left open to ambient background pressure of the vacuum chamber (10^{-4} to 5×10^{-4} torr), and the switch was "closed" by discharging four uniformly distributed Bendix surface igniter plugs into the interelectrode spacing of the switch. To preclude a potential across the electrode nozzle prior to switch activation, a large resistance was permanently connected across the two electrodes of the nozzle. Capacitor voltages ranging between 1 and 1.5 kv were examined during all of the studies reported herein, with discharge energies ranging roughly from 250 to 350 joules. Current traces of the main discharge were taken during accelerator operation with the switch shorted by a concentric shorting ring and were found to be essentially the same as when the switch was not shorted. A distortion of the current waveform, such as frequently encountered in low-pressure switches, was not observed. An electromagnetically driven valve† was used to inject gaseous propellant into the interelectrode spacing of the electrode nozzle. Only nitrogen was used as the propellant during the tests reported in the first part of this study. The upstream propellant supply pressure and the valve voltage were kept fixed at such values as to produce an electrical discharge for all imposed delays between propellant injection and voltage application. The accelerator assembly was mounted on a thrust stand, and thrust data was taken after the initial drop in thrust[1] as a function of the imposed time delay between valve activation (i.e., propellant injection) and engine voltage application.

Received January 5, 1965. This work was carried out under partial support of Contract No. NONR 4534 (00).

* Staff Engineer, Power Conversion Division. Member AIAA.

† Microvalve Model No. MV-12 AF, Space Sciences, Inc., Natick, Mass.